Relation between the 100 hPa heat flux and stratospheric potential vorticity

Yvonne B. L. Hinssen *

Institute for Marine and Atmospheric research Utrecht, Utrecht, The Netherlands

Maarten H. P. Ambaum

Department of Meteorology, University of Reading, United Kingdom

* *Corresponding author address:* Yvonne Hinssen Institute for Marine and Atmospheric research Utrecht, Utrecht University PO Box 80000, 3508 TA Utrecht, The Netherlands.

E-mail: y.b.l.hinssen@uu.nl

ABSTRACT

It is shown that a quantitative relation exists between the stratospheric polarcap potential vorticity and the 100 hPa eddy heat flux. A difference in potential vorticity between years is found to be linearly related to the flux difference integrated over time, taking into account a decrease in relaxation timescale with height in the atmosphere.

This relation (the PV-flux relation) is then applied to the 100 hPa flux difference between 2008/2009 and the climatology (1989-2008), to obtain a prediction of the polarcap potential vorticity difference between the 2008/2009 winter and the climatology. A prediction of the 2008/2009 polarcap potential vorticity is obtained by adding this potential vorticity difference to the climatological potential vorticity. The observed polarcap potential vorticity for 2008/2009 shows a large and abrupt change in the potential vorticity in midwinter, related to the occurrence of a major sudden stratospheric warming in January 2009, and this is also captured by the potential vorticity predicted from the 100 hPa flux and the PV-flux relation.

The results of the mean PV-flux relation as well as the 2009 case study show that, on average, about 50% of the interannual variablity in the state of the Northern Hemisphere stratosphere is determined by the variations in the 100 hPa heat flux. This explained variance can be as large as 80% for more severe events, as demonstrated for the 2009 major warming.

1. Introduction

Major sudden stratospheric warmings are phenomena during which the polar stratosphere is substantially warmed and the stratospheric winds reverse direction from westerlies to easterlies. These stratospheric changes can affect the tropospheric circulation directly through hydrostatic and geostrophic adjustment, or indirectly due to changes in the reflection and propagation of planetary waves.

Since the work of Charney and Drazin (1961) and Holton and Mass (1976), sudden stratospheric warmings are believed to be primarily forced from below by wave activity entering the stratosphere from the troposphere (see also Andrews et al. 1987). For example, Charlton and Polvani (2007) show that the 100 hPa heat flux (which is a measure of the upward propagating wave forcing to the stratosphere) is increased in the weeks before the occurrence of a sudden stratospheric warming. Here we examine to which extent the wave forcing of the stratosphere drives the large scale stratospheric variability in general, and the stratospheric variations accompanying the 2009 sudden stratospheric warming in particular.

First, we examine the relation between the stratospheric polar cap potential vorticity (PV) and the 100 hPa heat flux. The importance of such a relationship was highlighted in, for example, Ambaum and Hoskins (2002), who showed that stratospheric PV anomalies are important for the troposphere. They found a positive feedback loop between stratospheric PV anomalies and tropospheric circulation, mediated by upper tropospheric Eliassen-Palm fluxes.

The relation between poleward heat flux and stratospheric PV (the PV-flux relation) is based on the idea that a wave forcing can erode the stratospheric PV structure. The values of the Northern Hemisphere PV are for example much lower than those of the Southern Hemisphere PV, and it is generally known that wave propagation to the stratosphere plays a larger role in the Northern Hemisphere since the topography and land-sea configuration are more favorable for wave excitation in the Northern Hemisphere than in the Southern Hemisphere.

In the present study we will examine this PV-flux relation on a daily basis, using the European Centre for Medium-Range Weather Forecasts (ECMWF) ERA-interim reanalysis data from 1989 to 2008. Although it is often assumed that the 100 hPa heat flux is the driving force behind stratospheric variability, to our knowledge a PV-flux relation of the form presented here, directly relating a flux difference to a PV difference on a daily basis, has not been published before.

Secondly, we use this mean PV-flux relation to predict the daily 2008/2009 polar cap PV anomaly from the 2008/2009 100 hPa heat flux anomaly. Comparison of the predicted PV with the actual ERA-interim PV for the 2008/2009 winter then indicates to what extent the stratospheric PV can be predicted from the 100 hPa heat flux. The differences will also indicate the importance of other factors, such as those internal to the stratosphere.

The present work is related to that of Newman et al. (2001) and Austin et al. (2003), who present a relation between the winter heat flux and the spring polar temperatures, based on monthly timescales. In the present study this idea is applied to daily differences in PV and heat flux between different years in the Northern Hemisphere.

The physical basis of the PV-flux relation is described in section 2. Section 3 presents an overview of the data used and our definition of splitting the PV into a reference state and an anomaly. The procedure to find the mean PV-flux relation is given in section 4.

Section 5 presents the results of the 2009 sudden stratospheric warming case study and sensitivity studies are described in section 6. Finally, section 7 presents a discussion and some conclusions.

2. Physical basis

The PV-flux relation we use is derived from the zonal mean quasigeostrophic potential vorticity equation (e.g., James 1995). It reads

$$[q]_t + [v^\star q^\star]_y = [S], \tag{1}$$

where subscripts denote partial derivatives, square brackets denote zonal means, and the superscripts * denote deviations from the zonal mean. In the above equation, q is the quasigeostrophic potential vorticity (or pseudo-potential vorticity, see Hoskins et al. 1985), v is the meridional wind, and S is some diabatic source term on the quasigeostrophic potential vorticity. We use cartesian coordinates for simplicity of notation.

If we integrate this equation poleward of some given latitude y_0 (the polar cap in spherical coordinates) to find the average $\langle q \rangle$ over the polar cap northward of this latitude, then we get

$$\langle q \rangle_t = \langle S \rangle + L\,[v^\star\, q^\star](y_0), \tag{2}$$

with L the longitudinal extent of the domain at latitude y_0. In Eq. 2 we now replace the average source term by a Newtonian relaxation and we rewrite the poleward PV flux as the divergence of the Eliassen–Palm flux, $\boldsymbol{F}$,

$$\langle q \rangle_t = \frac{\langle q \rangle_R - \langle q \rangle}{\tau} + \frac{L}{\rho_R} \nabla \cdot \boldsymbol{F}(y_0). \tag{3}$$

Here $\langle q \rangle_R$ is the radiative equilibrium value of the polar cap mean PV, τ is the radiative timescale at the given level, and ρ_R is the reference density profile which is required in the quasigeostrophic framework.

We now make the assumption that the spatial structure of the Eliassen–Palm flux divergence does not vary, so that

$$\nabla \cdot \boldsymbol{F} = \phi(y, z)\, \chi(t), \tag{4}$$

where ϕ is the spatial structure function and χ its temporal modulation. This is a strong assumption, which can only be justified in hindsight by the success of our model (or lack thereof). However, some a priori justification is found in the fact that the linear paradigm of Rossby wave propagation on a background flow is defined for a fixed background, where the mean zonal state defines the refractive index for the waves. Our assumption further implies that the propagation of the Rossby waves (where the local group velocity is assumed to be parallel to $\boldsymbol{F}$) is immediate, which is in contradiction with observations (e.g., Harnik 2002). Nonetheless, the time scale of propagation is short enough for this assumption to be reasonably satisfied.

We can now express the time modulation $\chi(t)$ in terms of the mean poleward heat flux at the lower boundary of the domain. To this end, we integrate $\nabla \cdot \boldsymbol{F}$ over the whole stratosphere, with as lower boundary the 100 hPa level, for simplicity. Using Gauss' theorem, this integral can be expressed as a boundary integral for the Eliassen–Palm fluxes perpendicular to the boundaries. We assume that the meridional boundaries do not contribute to this integral (there are weak heat fluxes at the equatorward edge of the domain and there are, by definition, no meridional fluxes through the pole). We also assume that the notional top of the domain (this could be space, in principle) does not support strong upward Eliassen–Palm fluxes. We then find that the only contribution to the integral comes from the vertical Eliassen–Palm fluxes at the lower boundary. The integral is therefore proportional to the meridional average value of the 100 hPa poleward heat flux, that is,

$$\int_{\text{strat}} \nabla \cdot \boldsymbol{F} \, \mathrm{d}y \, \mathrm{d}z = \chi \int_{\text{strat}} \phi \, \mathrm{d}y \, \mathrm{d}z = - \int_{\text{lower bdy}} F^{(z)} \, \mathrm{d}y = f_0 W \rho_R \{[v^\star T^\star]\}_{100\text{hPa}} / T_R. \quad (5)$$

Here the two integrals are over the whole stratosphere in the meridional plane and its lower boundary, respectively. Further, $\{[v^\star T^\star]\}_{100\text{hPa}}$ is the meridional mean of the 100 hPa poleward heat flux, W the meridional extent of the lower boundary, f_0 a suitable reference value for the Coriolis parameter, and T_R a suitable reference temperature at 100 hPa. This result allows us to write χ as a function of the mean poleward heat fluxes at the lower boundary only,

$$\chi(t) = \frac{f_0 W \rho_R}{T_R \int_{\text{strat}} \phi \, \mathrm{d}y \, \mathrm{d}z} \{[v^\star T^\star]\}_{100\text{hPa}}. \quad (6)$$

With this expression for χ, we can rewrite Eq. 3 as

$$\langle q \rangle_t = \frac{\langle q \rangle_R - \langle q \rangle}{\tau} - A(z) \{[v^\star T^\star]\}_{100\text{hPa}}, \quad (7)$$

with the vertical structure function A given by

$$A(z) = \frac{f_0 W L}{T_R} \frac{\phi(y_0, z)}{\int_{\text{strat}} \phi \, \mathrm{d}y \, \mathrm{d}z}. \quad (8)$$

Equation 7 describes some well-known properties of the polar cap PV: it relaxes radiatively to some radiative equilibrium value and any poleward heat flux (upward Eliassen–Palm flux) at the lower boundary tends to decelerate the mean stratospheric wind and decrease the PV value at the poles.

Equation 7 contains only the polar cap PV and 100 hPa poleward flux. It can be straightforwardly solved as

$$\langle q\rangle(t) = \langle q\rangle(0)e^{-t/\tau} + \int_0^t \frac{\langle q\rangle_R(t-t')}{\tau} e^{-t'/\tau}dt' - A\int_0^t F(t-t')e^{-t'/\tau}dt', \tag{9}$$

where for brevity we write

$$F = \{[v^\star T^\star]\}_{100\mathrm{hPa}}. \tag{10}$$

The first term in Eq. 9 is the transient effect of the initial condition, the second term is the radiative contribution to the polar cap PV, and the last term represents the effect of waves on the polar cap PV.

After the initial transients have died away, the first two terms on the right hand side are the same every year as long as we investigate the same hemisphere. Furthermore, we start our integrations in the summer, so there are only small differences between the initial conditions anyway. Comparing two different years Y_1 and Y_2 on the same hemisphere therefore leaves us with an equation relating the PV difference between the years to the flux difference between the years:

$$\Delta_{Y_1Y_2}\langle q\rangle(t) = -A\int_0^t \Delta_{Y_1Y_2}F(t-t')e^{-t'/\tau}dt' \tag{11}$$

The relaxation timescale τ is related to the radiative timescales in the stratosphere and is height dependent, with an increasing timescale with decreasing height (e.g., Dickinson 1973). Therefore, the integrated flux difference is a function of height, even though the flux difference itself is not. In the next sections the Northern Hemisphere potential vorticity difference and time integrated flux difference are determined from the ERA-interim data for different year combinations for the years 1989 to 2008 and A is empirically determined. In what follows, the perturbation Ertel PV anomaly (which is defined in the next section) will be used to determine the relevant value for q.

3. Data

The ECMWF ERA-interim reanalysis dataset is used. This is the most recently produced reanalysis dataset, with an improved representation of the stratosphere compared to the previous ERA-40 reanalysis (Fueglistaler et al. 2009). The daily ERA-interim data (data from 12 UTC) of the zonal and meridional wind and the temperature for the January 1989 to June 2009 period are interpolated from isobaric to isentropic levels by the method described by Edouard et al. (1997). In order to make optimal use of the available ERA-interim data, a stretched grid in the vertical direction is employed. The isentropic potential vorticity Z_θ (Hoskins et al. 1985) is then calculated from:

$$Z_\theta = \frac{\zeta_\theta + f}{\sigma} \tag{12}$$

Here ζ_θ is the isentropic relative vorticity, f is the Coriolis parameter and σ is the isentropic density:

$$\zeta_\theta = -\frac{1}{a}\frac{\partial u}{\partial \phi} + \frac{u \tan\phi}{a} + \frac{1}{a\cos\phi}\frac{\partial v}{\partial \lambda} \tag{13}$$

$$\sigma = -\frac{1}{g}\frac{\partial p}{\partial \theta} \tag{14}$$

Here u is the zonal wind, v is the meridional wind, a is the radius of the Earth, ϕ is the latitude, λ is the longitude, p is the pressure, θ is the potential temperature and g is the gravitational acceleration. Zonal averaging and averaging over the 20-yr period 1989-2008 gives a dataset of zonal mean PV, zonal wind and pressure on isentropic levels. The domain of this dataset ranges from 90°N to 90°S in the horizontal, with a resolution of 1.5°, and from the Earth's surface to about 1250 K in the vertical, with a resolution varying from 1.7 K near the surface to about 10 K in the upper layers. The lower boundary of the domain is determined by the available data, and for each latitude this is defined as the first isentropic level for which data is available along the full latitude circle, meaning that the pressure is below 1000 hPa at all longitudes along this latitude circle. We will refer to this lower boundary as the 'surface', but it should be noted that this does not correspond to the actual surface of the Earth, but is located in the lower troposphere. This surface-isentropic level varies with latitude, during Northern Hemisphere winter from around 260 K at 90°N to about 310 K near the equator.

The zonal mean PV and the isentropic density are split into a reference state and an anomaly as follows:

$$Z_\theta \equiv Z_{\theta,\mathrm{ref}} + Z'_\theta; \sigma \equiv \sigma_{\mathrm{ref}} + \sigma' \tag{15}$$

with

$$Z_{\theta,\mathrm{ref}} = \frac{f}{\sigma_{\mathrm{ref}}} \tag{16}$$

and

$$\sigma_{\mathrm{ref}} = \frac{\int \sigma a \cos(\phi) d\phi}{\int a \cos(\phi) d\phi} \tag{17}$$

In other words, the reference isentropic density is the area-weighted average of σ over the domain in question. In our case we focus on the Northern Hemisphere and choose the area poleward of 10°N. Therefore, σ_{ref} depends only on the height (θ). The PV anomaly, Z'_θ, represents that part of the PV field that induces a wind field, according to the PV inversion equation (see e.g., Hinssen et al. 2010).

The polarcap PV anomaly is defined as the area weighted average of the PV anomaly poleward of 70°N. We consider a year running from July to June the next year. With the year 2008/2009 we thus mean the period July 2008 to June 2009.

The meridional wind and temperature fields on pressure levels are used to determine the zonal mean heat flux, $[v^{\star}T^{\star}]$, with the brackets denoting a zonal mean and the stars a deviation from zonal mean. The 100 hPa heat flux is often used as a measure of the wave forcing from the troposphere to the stratosphere (e.g., Waugh et al. 1999; Polvani and Waugh 2004; Charlton et al. 2007). Since most planetary wave activity crosses the 100 hPa level between 40° and 80° degrees (see for example Fig. 2 in Charlton et al. 2007), we use the area weighted average of the 100 hPa heat flux between 40°N and 80°N as a measure of wave forcing from the troposphere to the stratosphere. This quantity is determined for each day of each year. A more detailed discussion of the heat flux can be found in Newman and Nash (2000).

4. The climatological PV-flux relation

First a mean relaxation timescale τ is determined as a function of potential temperature. There are 171 different year combinations, the first being 1989/1990 - 1990/1991 and the last 2006/2007 - 2007/2008 (we only examine different year combinations, so if 1989/1990 - 1990/1991 is examined, 1990/1991 - 1989/1990 is not, as it provides no new information).

For each year combination the polarcap PV anomaly difference and flux difference are determined. The flux difference is then integrated from day zero (the first of July) to day t to determine the integral on the right hand side of Eq. 11 as a function of t (day of the year) and τ for each year combination. The covariance between the integrated flux difference and minus the polarcap PV anomaly difference is determined for the time period December to March (DJFM) as a function of τ and θ (minus the PV values are only used to obtain a positive correlation, and eventually positive values for A in Eq. 11). The variance of the polarcap PV anomaly difference as a function of θ and the variance of the integrated flux difference as a function of τ are determined for the same period. The months December to March are chosen because the influence of waves on the stratosphere is largest in the winter season, since waves can only propagate to the stratosphere when the winds are westerly (Charney and Drazin 1961). The mean covariance and variances over all year combinations are then calculated, and these are used to determine a mean DJFM correlation coefficient as a function of τ and θ.

The mean τ as a function of height is then found by determining for which τ the correlation coefficient is 95 % of its maximum value at each level. We do not use the actual maximum value, since in the lower stratosphere the correlation coefficient is found to increase with increasing τ to values of τ exceeding 200 days, while a correlation of 95 % is obtained at much lower values of τ. The resulting τ and accompanying correlation are given in Figure 1. The value of τ increases from about 10 days in the upper levels, to about one month near 700 K and three months around 500 K.

Figure 1 also shows that for the lower to middle stratosphere the mean correlation coefficient is about 0.7. This indicates that Eq. 11 may indeed provide a reasonable predictive model for the polarcap PV. These values of the correlation coefficient indicate the about 50% of the variance in the polarcap PV can be predicted from the preceding 100 hPa heat flux.

Examples of the integrated flux difference and minus the polarcap PV anomaly difference as a function of time on the 600 K level are given in Figure 2 for the year combinations 1994/1995 - 1996/1997, 1998/1999 - 2000/2001 and 2003/2004 - 2004/2005. Here the optimal value of τ from Figure 1 was used. Figure 2 shows that there is a strong relation between the flux difference and PV anomaly difference in general, although not all variations in PV anomaly are accompanied by a flux variation, consistent with the correlation values of Figure 1.

To determine a general PV-flux relation based on all year combinations, all DJFM flux differences and minus polarcap PV anomaly differences are determined. The -PV anomaly differences versus flux differences are shown for the 600 K level in Figure 3a, and a linear fit is plotted through the data. This can be done for each isentropic level, and the slope (A in Eq. 11) as a function of θ is given in Figure 3b. The assumption behind Eq. 11 is that a flux difference of zero is accompanied by a zero PV anomaly difference and it is indeed found that the best linear fit through the data nearly crosses through the (0,0) point (see Figure 3a for the 600 K level).

We have determined a mean PV-flux relation based on ERA-interim data for the period July 1989 to June 2008. The general form of the PV-flux relation is given by Eq. 11. The values of τ and A (both as a function of θ) have been determined from the 1989-2008 data, and can now be applied to any 100 hPa flux difference to obtain a PV anomaly difference. The PV-flux relation on the 600 K level as visualized in Figure 3a, shows that interannual variations in the polarcap PV anomaly are to a good approximation linearly related to the interannual variations in the integrated 100 hPa heat flux.

5. The PV-flux relation applied to the 2008/2009 winter

The mean PV-flux relation is now used to predict the polarcap PV anomaly from the 100 hPa heat flux for the 2008/2009 winter. This is an independent test case, since the 2008/2009 data is not used in the determination of the general PV-flux relation. Applying the PV-flux relation to the 2008/2009 flux therefore presents a test on how well the variation in the polarcap PV anomaly can be predicted from the variation in the 100 hPa heat flux. The polarcap PV anomaly for 2008/2009 is given in Figure 4a, clearly showing the drop in stratospheric polarcap PV anomaly during the sudden stratospheric warming in late January (24 January 2009 according to Labitzke and Kunze 2009). For comparison: the 1989-2008 climatological stratospheric polarcap PV anomaly (Figure 4b) is positive throughout the whole winter season. Comparison of the climatological and 2008/2009 (not integrated) 100 hPa heat flux (Figure 5) shows that during the second half of January 2009 the flux was about three times as large as the climatological flux, indicating that the wave forcing of the stratosphere was exceptionally large.

We apply the PV-flux relation to the 2008/2009 winter with respect to the climatology, and thus use the difference in flux between 2008/2009 and the climatology. Eq. 11 is used to calculate the PV anomaly difference from the flux difference, using the mean τ

and A determined in the previous section. The 2008/2009 polarcap PV anomaly is then predicted by adding this PV anomaly difference to the climatological polarcap PV anomaly. The result is shown in Figure 6a. At first sight the predicted polarcap PV anomaly looks very similar to the ERA-interim polarcap PV anomaly (Figure 4a), with as most striking feature the sudden stratospheric warming, accompanied by a change in sign of the polarcap PV anomaly in the second half of January. Other similarities between the predicted and ERA-interim PV anomaly are the increasing stratospheric PV anomaly values in autumn as the pole cools, the recovery of the positive polarcap PV anomaly values after the sudden stratospheric warming, starting in the upper stratosphere and extending downward in time (due to the longer relaxation timescales in the lower stratosphere compared to the upper stratosphere), but not reaching the lower stratosphere before the final break up of the vortex in spring.

The main differences between the predicted and ERA-interim polar PV anomaly are a too small variability in early winter for the predicted PV anomaly, and some differences in the timing and amplitude of the recovery of the PV anomaly after the sudden stratospheric warming. However, in general it can be concluded that the predicted polarcap PV anomaly captures the main features and large scale variability of the actual PV anomaly quite well.

This is supported by Figure 6b, which shows a cross section at 600 K of the predicted polarcap PV anomaly for 2008/2009, the ERA-interim polarcap PV anomaly for 2008/2009 and the climatological polarcap PV anomaly. The 600 K polarcap PV anomaly values show that the predicted PV anomaly captures the high values before the sudden stratospheric warming, the quick decrease during the sudden stratospheric warming and the slow recovery afterwards. The clear resemblance between the predicted and ERA-interim polarcap PV anomaly is also visible in Figure 7, which shows the zero contour of the daily polarcap PV anomaly as a function of time and potential temperature for the climatology, ERA-interim 2008/2009 case and the predicted 2008/2009 case, indicating the structure of the formation and break up of the polar vortex. This figure also shows that, although the recovery of the PV anomaly after the sudden stratospheric warming is somewhat different for the predicted case compared to the ERA-interim data, the break up of the vortex for the predicted case is later than for the climatology and the structure of the predicted PV anomaly is clearly closer to the observed structure than to the climatology.

The good agreement between the predicted and actual polarcap PV anomaly indicates that, for the 2009 case, the information for the sudden stratospheric warming was already present in the 100 hPa heat flux. A supporting result is obtained by Kinnersley (1998) in a model study. For the winter of 1987/1988 Kinnersley (1998) finds that the state of the extratropical stratosphere during this winter is hardly influenced by the phase of the QBO, while it strongly depended on the planetary wave forcing from the lower stratosphere.

Figures 6 and 7 thus show that it is possible to predict the polarcap PV anomaly for 2008/2009 from just the 2008/2009 100 hPa heat flux, together with the climatological polarcap PV anomaly and flux, and the mean PV-flux relation.

6. Sensitivity studies

In this section the sensitivity of the results presented in section 5 to the choice of the relaxation timescale τ and to the slope of the PV-flux relation (A in Eq. 11) is studied.

a. *Sensitivity of the predicted PV anomaly to the value of the slope*

The results presented in the previous section are based on the general PV-flux relation as given by Eq. 11, with the slope A empirically determined in section 4. However, Figure 3a shows quite some scatter of the data around the linear fit. Therefore we study the sensitivity of the results presented in the previous section to the value of the slope, by repeating the estimation of the 2008/2009 polarcap PV anomaly from the PV-flux relation, with a 50% increased or decreased slope. The values of τ are kept at the values obtained in section 4. The observed 2008/2009 polarcap PV anomaly is shown in Figure 8, together with the predicted polarcap PV anomaly with the slope A as presented in Figure 3b and with a slope of $0.5 * A$ and $1.5 * A$, with a larger drop in PV anomaly during the sudden stratospheric warming for a larger slope. Figure 8a shows the results on the 600 K level, while Figure 8b presents the zero contours of the observed and predicted polarcap PV anomaly as a function of potential temperature. Figure 8 indicates that the slope determines the value of the PV anomaly minimum during the sudden stratospheric warming.

b. *Sensitivity of the predicted PV anomaly to the value of* τ

The value of the relaxation timescale τ also plays an important role in the PV-flux relation. Therefore we also examine the sensitivity of the results presented in section 5 to variations in τ. The value of τ is increased or decreased by 50%, after which the procedure described in section 4 is repeated to obtain the accompanying slope values. The polarcap PV anomaly is then predicted again from Eq. 11 with the new values for τ and A. The observations and different predictions of the 2008/2009 polarcap PV anomaly are shown in Figure 9a for the 600 K level, and in Figure 9b for the zero contours as a function of potential temperature. Figure 9 illustrates that the value of τ determines the speed and strength of the recovery of the PV anomaly after the sudden stratospheric warming, where the recovery is less strong and takes longer for a larger τ, as you would expect. The results for the 2008/2009 winter are, however, not very sensitive to variations in τ.

Another way to obtain an estimate for the relaxation timescale, is by approximating τ as a linear function of $\ln(\theta)$ (with θ in Kelvin). Assuming $\tau = 5$ days at 1600 K (at a height of about 40 km) and $\tau = 90$ days at 300 K (comparable to the damping timescales mentioned in Newman et al. 2001, to give good correlations between the heat flux and polar temperatures), τ is given by:

$$\tau = -50\ln(\theta) + 375. \tag{18}$$

The value of τ as a function of potential temperature obtained from Eq. 18 is presented in Figure 10, together with the correlation coefficient that accompanies this τ (found by inserting this τ into the correlation coefficient obtained in section 4. Note that due to the logarithmic scaling of the vertical axis τ is a straight line in Figure 10. The correlation coefficient for this τ is very similar to the correlation found for the mean τ in section 4 (Figure 1). This τ is now used to obtain a general PV-flux relation, following the method described in section 4, after which the values for the slope and τ are applied to predict the PV anomaly difference between 2008/2009 and the climatology. The 2008/2009 polarcap PV anomaly is then determined by adding this PV anomaly difference to the climatological polarcap PV anomaly, and the results are shown in Figure 11a for the 600 K level and in Figure 11b for the structure of the polarcap PV anomaly as a function of potential temperature. The results are very similar to those presented in Figure 6b and Figure 7 for the τ determined from the ERA-interim data, again showing that the results for 2008/2009 are not very sensitive to the choice of τ.

7. Conclusions

We have shown that a quantitative, predictive relation exists between the stratospheric polarcap PV anomaly and the 100 hPa heat flux. A difference in PV anomaly is found to be linearly related to the integrated flux difference, with an integration over time of the flux difference times a factor $\exp(-t/\tau)$, to include the effect of decreasing relaxation timescales with height. This general PV-flux relation was then applied to the 100 hPa flux difference between 2008/2009 and the climatology (1989-2008), to obtain a prediction of the polarcap PV anomaly difference between the 2008/2009 winter and the climatology. A prediction of the 2008/2009 polarcap PV anomaly was obtained by adding this PV anomaly difference to the climatological PV anomaly. The ERA-interim polarcap PV anomaly for 2008/2009 shows a large and abrupt change in the PV anomaly in midwinter, related to the occurrence of the sudden stratospheric warming, and this is also captured by the PV anomaly predicted from the 100 hPa flux and the PV-flux relation.

The results of the general PV-flux relation show that, on average, about 50% of the interannual variability in the state of the stratosphere that is observed in the Northern Hemisphere can be explained by the interannual variations in the 100 hPa heat flux. For the individual winter of 2008/2009, the fraction of the variability explained by the 100 hPa heat flux was even larger ($\sim 80\%$). This is consistent with the conclusion of Christiansen (2001), who found that the stratospheric variability is driven by the vertical component of the Eliassen-Palm flux (which is proportional to the heat flux used in the present study) based on covariance analyses.

Furthermore, we conclude that for the 2009 sudden stratospheric warming the information for the sudden stratospheric warming was already present in the 100 hPa heat flux, indicating that the state of the upper stratosphere prior to the sudden stratospheric warming was of minor importance for the occurrence of the sudden stratospheric warming. Previous studies have shown that before the occurrence of sudden stratospheric warmings the stratosphere is often in a preconditioned state, with a poleward displaced polar jet (Labitzke 1981; Limpasuvan et al. 2004). This corresponds to a steeper PV gradient near the pole, allowing for stronger vertical wave propagation and stronger erosion of the polar vortex (Polvani and Saravanan 2000; Scott et al. 2004). Although a steep stratospheric PV gradient at a more poleward location than for the climatology was indeed present in early January 2009, this is only of secondary importance for our study, since we predicted the polarcap PV anomaly for the 2008/2009 winter from just the climatological PV (which is not preconditioned), the mean PV-flux relation and the 2008/2009 100 hPa heat flux. So the state of the upper stratosphere in 2008/2009 is not needed to obtain a reasonable prediction of the polarcap PV anomaly.

However, the state of the lower stratosphere before the sudden stratospheric warming could be of importance in determining the amount of wave activity that can propagate into the stratosphere, thereby influencing the 100 hPa flux. In a model study, Scott and Polvani (2004) indeed find that sudden stratospheric warming-like variability in the stratosphere may exist in the absence of tropospheric variability. Bell (2009) further shows that the increased wave driving of the stratosphere that is found for enhanced greenhouse gas concentrations can partly be attributed to increased tropospheric wave generation, but that changes in the radiative state of the stratosphere are also important. Haklander et al. (2007), on the other hand, show that the interannual variability of the 100 hPa heat flux is dominated by stationary waves (which are excited in the troposphere). Furthermore, transient wave excitation is abundant in the troposphere, so that it is realistic to assume that the 100 hPa heat flux is influenced by tropospheric waves. This is supported by the 2008/2009 heat flux at 850 hPa (not shown), which also shows a peak in January, a few days before the peak at 100 hPa. We therefore believe that at least part of the variability in the 100 hPa heat flux is related to wave forcing from the troposphere to the stratosphere, but can not exclude a dependence of the 100 hPa flux on the state of the lower stratosphere in the present study.

Smaller scale stratospheric variability, as seen in December 2008 in Figure 4a, is only partly captured in the PV anomaly predicted from the 100 hPa flux, and might thus be due to stratospheric internal variability.

Sensitivity studies show that the results for the 2008/2009 predicted polarcap PV anomaly are not very sensitive to the values of the slope A of the general PV-flux relation (Eq. 11) or to the values of the relaxation timescale τ. Changes of $\pm$ 50% in A or τ hardly affect the qualitative results. The value of A influences the value of the PV anomaly minimum during the sudden stratospheric warming, where a higher A leads to a stronger decrease in PV anomaly during the sudden stratospheric warming. The values of τ, on the other hand, influences the recovery of the PV anomaly after the sudden stratospheric warming, with a faster and stronger recovery for a smaller τ.

The occurrence of a sudden stratospheric warming and its effect on the stratosphere depend on the climatological state of the stratosphere, although the stratospheric climate itself is also partly set by the presence of sudden stratospheric warmings. Nonetheless, our study implies that the occurrence or strength of sudden stratospheric warmings might change due to climate change. If, for example, diabatic cooling of the stratosphere due to increased greenhouse gas concentrations increases the climatological PV, the same wave forcing will lead to a less severe disturbance of the polar vortex, and the criterion of a major sudden stratospheric warming might not be met. Since the PV-flux relation as applied to 2008/2009 directly links the climatology and the wave forcing, the PV-flux relation framework might be a useful tool to examine the influence of climate change on the occurrence of sudden stratospheric warmings. It should, however, be noted that changes in the PV-flux relation should then also be taken into account.

Similar to its application to climate change studies, the PV-flux relation can be used to evaluate the ability of models to simulate realistic sudden stratospheric warmings (see Maycock et al. 2009, for a discussion about the inability of some seasonal forecasting models to simulate realistic sudden stratospheric warmings). Three aspects of the model climate can be compared to, for example, the ERA-interim climate. The first is the 100 hPa heat flux, representing the forcing of the stratosphere. The second is the polarcap PV anomaly distribution of the stratosphere, representing the state of the stratosphere. The third aspect is the PV-flux relation, representing the coupling between the troposphere and the stratosphere. The present PV-flux relation provides a useful framework in which to diagnose the performance of models with respect to stratospheric warmings.

Acknowledgments.

The ECMWF ERA-interim data used in this study have been provided by ECMWF.

REFERENCES

Ambaum, M. H. P. and B. J. Hoskins, 2002: The NAO troposphere-stratosphere connection. *J. Climate*, **15**, 1969–1978.

Andrews, D. G., J. R. Holton, and C. B. Leovy, 1987: *Middle atmosphere dynamics*. Academic Press, 489 pp.

Austin, J., et al., 2003: Uncertainties and assessments of chemistry-climate models of the stratosphere. *Atmos. Chem. Phys.*, **3 (1)**, 1–27.

Bell, C. J., 2009: The role of stratospheric variability in climate. Ph.D. thesis, University of Reading, UK.

Charlton, A. J. and L. M. Polvani, 2007: A new look at Stratospheric Sudden Warmings. Part I: Climatology and modeling benchmarks. *J. Climate*, **20**, 449–469.

Charlton, A. J., et al., 2007: A new look at stratospheric sudden warmings. Part II: Evaluation of numerical model simulations. *J. Climate*, **20**, 470–488.

Charney, J. G. and P. G. Drazin, 1961: Propagation of planetary-scale disturbances from the lower into the upper atmosphere. *J. Geophys. Res.*, **66 (1)**, 83–109.

Christiansen, B., 2001: Downward propagation of zonal mean zonal wind anomalies from the stratosphere to the troposphere: Model and reanalysis. *J. Geophys. Res.*, **106 (D21)**, 27 307–27 322.

Dickinson, R. E., 1973: Method of Parameterization for Infrared Cooling between Altitudes of 30 and 70 Kilometers. *J. Geophys. Res.*, **78**, 4451–4457.

Edouard, S., R. Vautard, and G. Brunet, 1997: On the maintenance of potential vorticity in isentropic coordinates. *Quart. J. Roy. Meteor. Soc.*, **123**, 2069–2094.

Fueglistaler, S., B. Legras, A. Beljaars, J. J. Morcrette, A. Simmons, A. M. Tompkins, and S. Uppala, 2009: The diabatic heat budget of the upper troposphere and lower/mid stratosphere in ECMWF reanalyses. *Quart. J. Roy. Meteor. Soc.*, **135**, 21–37.

Haklander, A. J., P. C. Siegmund, and H. M. Kelder, 2007: Interannual variability of the stratospheric wave driving during northern winter. *Atmos. Chem. Phys.*, **7**, 2575–2584.

Harnik, N., 2002: The evolution of a stratospheric wave packet. *J. Atmos. Sci.*, **59**, 202–217.

Hinssen, Y., A. van Delden, T. Opsteegh, and W. de Geus, 2010: Stratospheric impact on tropospheric winds deduced from potential vorticity inversion in relation to the Arctic Oscillation. *Quart. J. Roy. Meteor. Soc.*, **136**, 20–29.

Holton, J. R. and C. Mass, 1976: Stratospheric Vacillation Cycles. *J. Atmos. Sci.*, **33**, 2218–2225.

Hoskins, B. J., M. E. McIntyre, and A. W. Robertson, 1985: On the use and significance of isentropic potential vorticity maps. *Quart. J. Roy. Meteor. Soc.*, **111**, 877–946.

James, I. N., 1995: *Introduction to Circulating Atmospheres.* Cambridge University Press, 444 pp.

Kinnersley, J. S., 1998: Interannual variability of stratospheric zonal wind forced by the northern lower-stratospheric large-scale waves. *J. Atmos. Sci.*, **55**, 2270–2283.

Labitzke, K., 1981: The amplification of height wave 1 in January 1979: A characteristic precondition for the major warming in February. *Mon. Wea. Rev.*, **109**, 983–989.

Labitzke, K. and M. Kunze, 2009: On the remarkable Arctic winter in 2008/2009. *J. Geophys. Res.*, **114 (D00102)**, doi:10.1029/2009JD012273.

Limpasuvan, V., D. W. J. Thompson, and D. L. Hartmann, 2004: The life cycle of the northern hemisphere sudden stratospheric warmings. *J. Climate*, **17**, 2584–2596.

Maycock, A. C., S. P. E. Keeley, A. J. Charlton-Perez, and F. J. Doblas-Reyes, 2009: Stratospheric circulation in seasonal forecasting models: Implications for seasonal prediction. *Climate Dyn.*, doi:10.1007/s00382-009-0665-x.

Newman, P. A. and E. R. Nash, 2000: Quantifying the wave driving of the stratosphere. *J. Geophys. Res.*, **105 (D10)**, 12 485–12 497.

Newman, P. A., E. R. Nash, and J. E. Rosenfield, 2001: What controls the temperature of the Arctic stratosphere during the spring? *J. Geophys. Res.*, **106 (D17)**, 19 999–20 010.

Polvani, L. M. and R. Saravanan, 2000: The three-dimensional structure of breaking rossby waves in the polar wintertime stratosphere. *J. Atmos. Sci.*, **57**, 3663–3685.

Polvani, L. M. and D. W. Waugh, 2004: Upward wave activity flux as a precursor to extreme stratospheric events and subsequent anomalous surface weather regimes. *J. Climate*, **17**, 3548–3554.

Scott, R. K., D. G. Dritschel, L. M. Polvani, and D. W. Waugh, 2004: Enhancement of rossby wave breaking by steep potential vorticity gradients in the winter stratosphere. *J. Atmos. Sci.*, **61**, 904–918.

Scott, R. K. and L. M. Polvani, 2004: Stratospheric control of upward wave flux near the tropopause. *Geophys. Res. Lett.*, **31 (L02115)**, doi:10.1029/2003GL017965.

Waugh, D. W., W. J. Randel, S. Pawson, P. A. Newman, and E. R. Nash, 1999: Persistence of the lower stratospheric polar vortices. *J. Geophys. Res.*, **104 (D22)**, 27 191–27 201.

List of Figures

11 (a) Daily 2008/2009 polarcap PV anomaly (PVU) on the 600 K isentrope for the climatological PV anomaly (dotted), ERA-interim PV anomaly (dark grey) and predicted PV anomaly (with the relaxation timescale τ as in Eq. 18, light grey) as a function of time. (b) Daily polarcap PV anomaly (PVU) for the 1989-2008 ERA-interim climatology (dotted), for the 2008/2009 ERA-interim data (dark grey) and for 2008/2009 predicted from the climatological polarcap PV anomaly and the 2008/2009 - climatology 100 hPa heat flux difference, with τ as in Eq. 18 (light grey) as a function of potential temperature (K) and time. Only the zero contour is shown. In (a) 24 January is indicated by a vertical line. 41

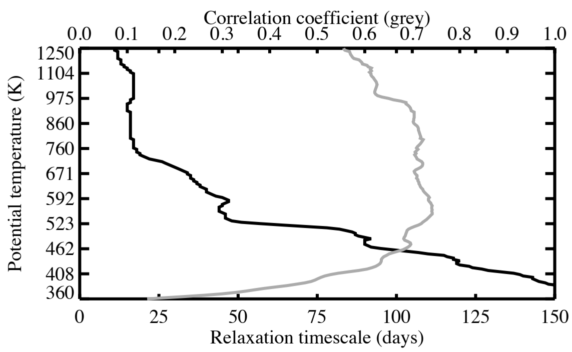

FIG. 1. Mean relaxation timescale τ (in days, bottom axis, black line) and mean correlation coefficient between DJFM integrated flux difference and minus DJFM polarcap PV anomaly difference (top axis, grey line) for this τ, both as a function of potential temperature (K). Note the logarithmic scaling of the potential temperature axis in this and following figures.

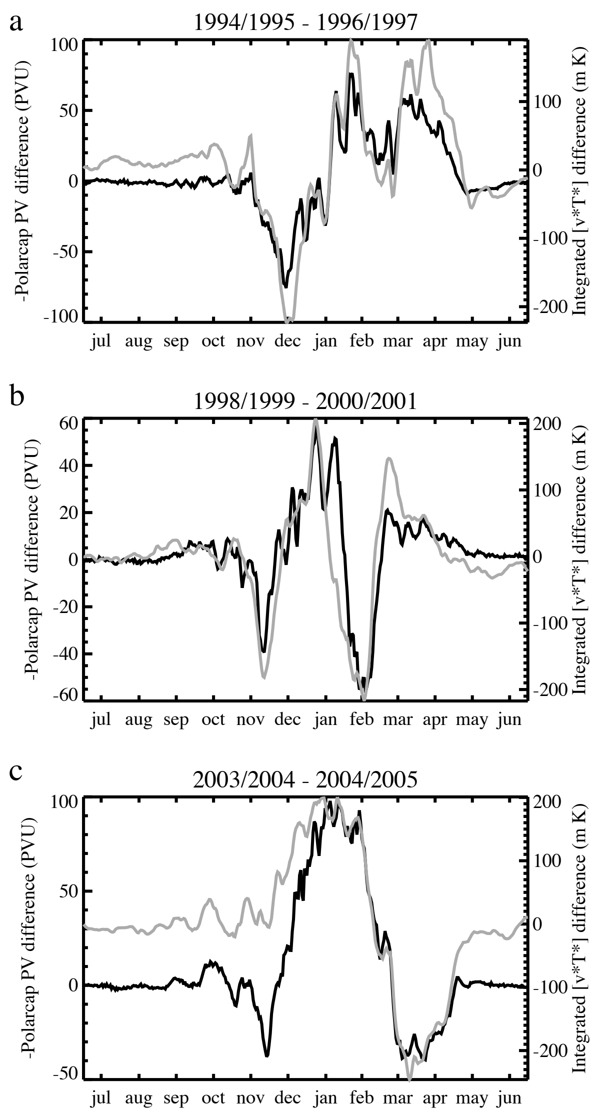

FIG. 2. Daily minus polarcap PV anomaly difference (in PVU, 1 PVU = 10^{-6} K m^2 kg^{-1} s^{-1}, left axis, black line) and daily integrated flux difference (in m K, right axis, grey line), both on the 600 K isentrope, as a function of time for the year combinations (a) 1994/1995 - 1996/1997, (b) 1998/1999 - 2000/2001 and (c) 2003/2004 - 2004/2005. The tickmarks indicate the middle of each month.

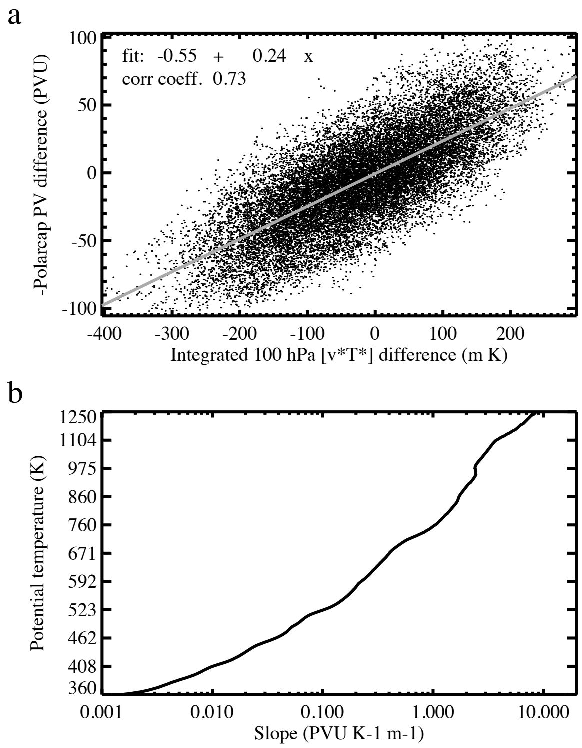

FIG. 3. (a) Minus polarcap PV anomaly differences (PVU) against integrated flux differences (m K) at 600 K for the months December to March, for all year combinations (points), and a linear fit through the data (line). (b) Slope (PVU K^{-1} m^{-1}) of the linear fit as a function of potential temperature, note the logarithmic scaling on both axes.

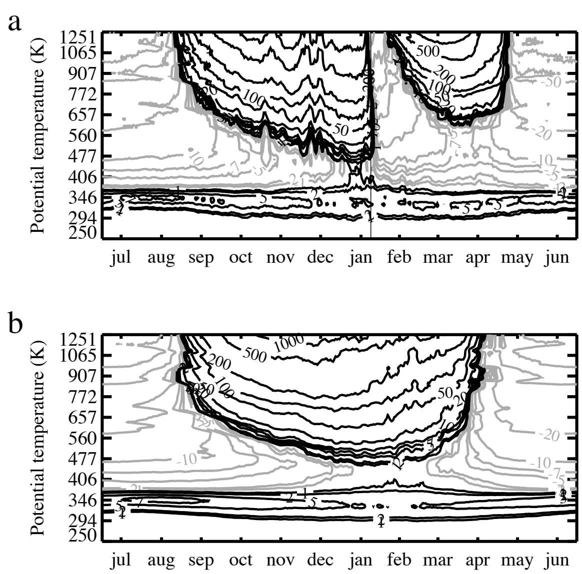

FIG. 4. Daily polarcap PV anomaly (PVU) for (a) July 2008 to June 2009 and (b) the 1989-2008 climatology, as a function of potential temperature (K) and time. Contours at 1, 2, 5, 7, 10, 20, 50, 100, 200, 500, 1000, 2000, 3000 PVU and negative values represented by grey lines. In (a) 24 January is indicated by a vertical line.

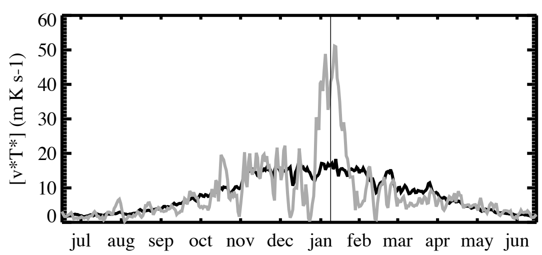

FIG. 5. Daily 100 hPa heat flux, $[v^{\star}T^{\star}]$ (in K m s^{-1}), as a function of time for the climatology (black) and 2008/2009 (grey). 24 January is indicated by a vertical line.

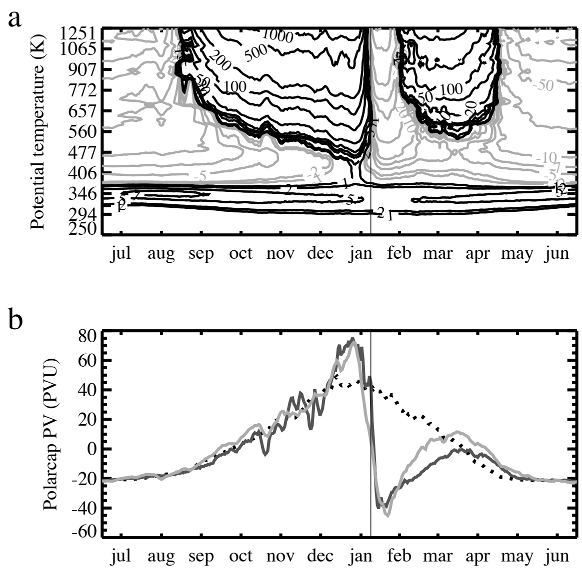

FIG. 6. (a) Predicted 2008/2009 daily polarcap PV anomaly (PVU) as a function of potential temperature (K) and time, contours as in Figure 4. (b) Daily 2008/2009 polarcap PV anomaly (PVU) on the 600 K isentrope for the predicted (light grey), ERA-interim (dark grey) and climatological (dotted) PV anomaly as a function of time. 24 January is indicated by a vertical line.

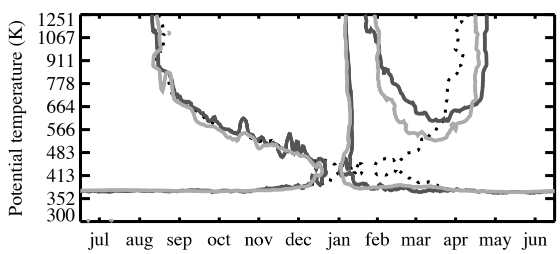

Fig. 7. Daily polarcap PV anomaly (PVU) for the 1989-2008 ERA-interim climatology (dotted), for the 2008/2009 ERA-interim data (dark grey) and for 2008/2009 predicted from the climatological polarcap PV anomaly and the 2008/2009 - climatology 100 hPa heat flux difference (light grey) as a function of potential temperature (K) and time. Only the zero contour is shown.

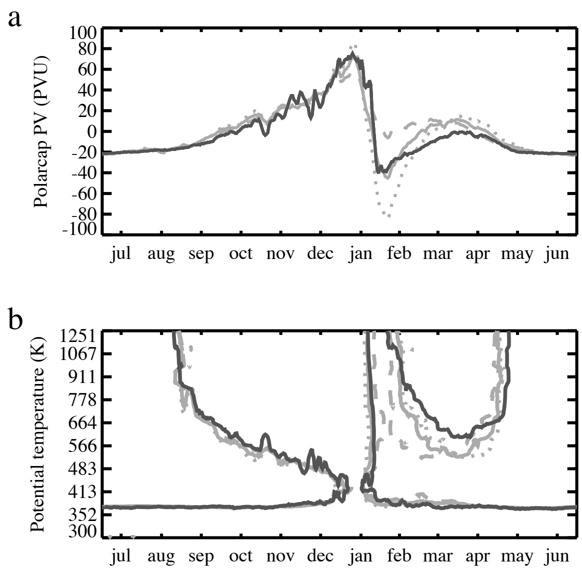

FIG. 8. (a) Daily 2008/2009 polarcap PV anomaly (PVU) on the 600 K isentrope for the ERA-interim polarcap PV anomaly (dark grey) and for the predicted polarcap PV anomaly (light grey) with slopes A (solid), $0.5*A$ (dashed) and $1.5*A$ (dotted), as a function of time. (b) Daily polarcap PV anomaly (PVU) for the 2008/2009 ERA-interim data (dark grey) and for 2008/2009 predicted from the climatological polarcap PV anomaly and the 2008/2009 - climatology 100 hPa heat flux difference with slopes A (light grey, solid), $0.5*A$ (light grey, dashed) and $1.5*A$ (light grey, dotted) as a function of potential temperature (K) and time. Only the zero contour is shown.

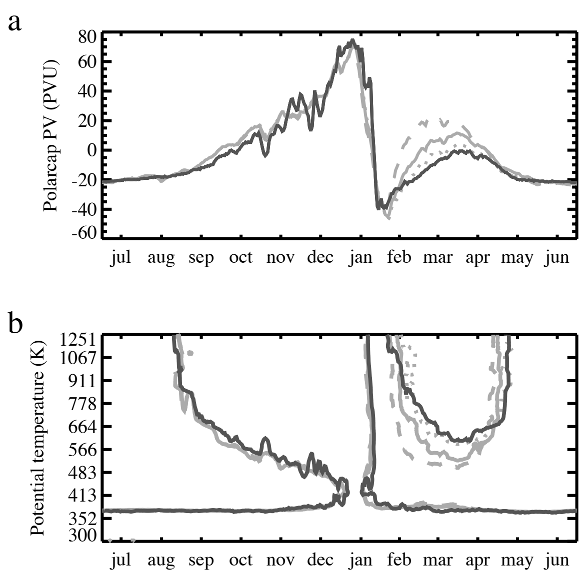

Fig. 9. (a) Daily 2008/2009 polarcap PV anomaly (PVU) on the 600 K isentrope for the ERA-interim polarcap PV anomaly (dark grey) and for the predicted polarcap PV anomaly (light grey) with relaxation timescales τ (solid), $0.5 * \tau$ (dashed) and $1.5 * \tau$ (dotted), as a function of time. (b) Daily polarcap PV anomaly (PVU) for the 2008/2009 ERA-interim data (dark grey) and for 2008/2009 predicted from the climatological polarcap PV anomaly and the 2008/2009 - climatology 100 hPa heat flux difference with timescales τ (light grey, solid), $0.5 * \tau$ (light grey, dashed) and $1.5 * \tau$ (light grey, dotted) as a function of potential temperature (K) and time. Only the zero contour is shown.

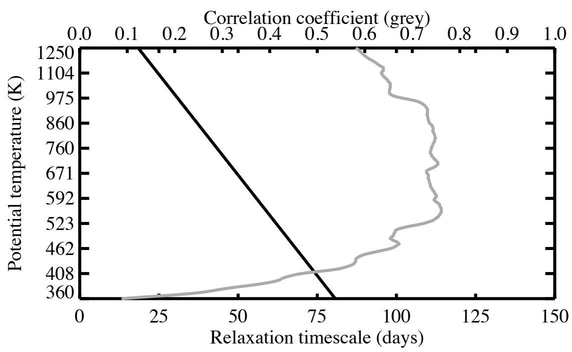

FIG. 10. Predicted relaxation timescale: $\tau = -50\ln(\theta) + 375$ (in days, bottom axis, black line) and corresponding correlation coefficient between DJFM integrated flux difference and minus DJFM polarcap PV anomaly difference derived from the ERA-interim data 1989-2008 (top axis, grey line), both as a function of potential temperature (K). Note the logarithmic scaling of the potential temperature axis.

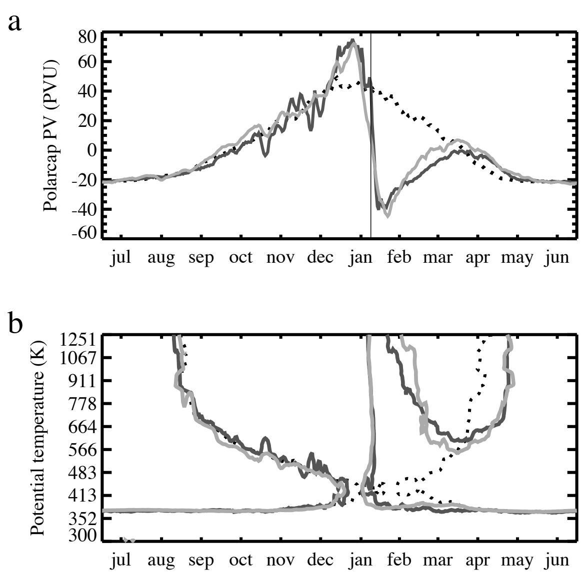

FIG. 11. (a) Daily 2008/2009 polarcap PV anomaly (PVU) on the 600 K isentrope for the climatological PV anomaly (dotted), ERA-interim PV anomaly (dark grey) and predicted PV anomaly (with the relaxation timescale τ as in Eq. 18, light grey) as a function of time. (b) Daily polarcap PV anomaly (PVU) for the 1989-2008 ERA-interim climatology (dotted), for the 2008/2009 ERA-interim data (dark grey) and for 2008/2009 predicted from the climatological polarcap PV anomaly and the 2008/2009 - climatology 100 hPa heat flux difference, with τ as in Eq. 18 (light grey) as a function of potential temperature (K) and time. Only the zero contour is shown. In (a) 24 January is indicated by a vertical line.